Asian Journal of Chemistry; Vol. 37, No. 9 (2025), 2169-2175
ASIAN JOURNAL OF CHEMISTRY
https://doi.org/10.14233/ajchem.2025.34203

Green One-Pot Synthesis, Docking, ADMET and Antibacterial Evaluation of 1,4-Dihydropyrano[2,3-*c*]pyrazole Derivatives

P. SIVADHARANI and S.R. JAYAPRADHA*

P.G. and Research Department of Chemistry, Government Arts College for Women (Affiliated to Mother Teresa Women's University, Kodaikanal), Nilakottai-624208, India

*Corresponding author: E-mail: srjayapradha2023@gmail.com

Received: 6 June 2025 *Accepted*: 21 July 2025 *Published online*: 30 August 2025 AJC-22096

Environmentally benign, time-efficient and straightforward methodologies have been developed for the synthesis of fused pyranopyrazole derivatives *via* a one-pot four-multicomponent reaction (MCR). Two synthetic approaches were employed using aromatic aldehydes, ethyl acetoacetate, malononitrile and hydrazine hydrate with L-histidine serving as an effective organocatalyst. **In method I**, the reaction was carried out in aqueous medium at 85 ºC, affording the desired product with a yield of 93%. In **method II**, a solvent-free approach utilizing different mole ratio of the same catalyst achieved a comparable yield of 92% within 5 min, demonstrating the efficiency of the protocol. The structures of the synthesized pyranopyrazole derivatives were confirmed using spectroscopic techniques including UV, FT-IR, ^{1}H NMR and ^{13}C NMR. The physico-chemical and pharmacokinetic properties were evaluated using the freely accessible SwissADME web server. Furthermore, molecular docking studies were performed using AutoDock and Molegro Molecular Viewer to assess the binding interactions of the synthesized compounds with glucosamine-6-phosphate synthase (GlmS), a validated antibacterial target. The docking results suggest the potential inhibitory activity against several tested bacterial strains.

Keywords: Pyranopyrazoles, L-Histidine, Water, Solvent-free method, Docking studies.

INTRODUCTION

Pyranopyrazoles are the fused heterocyclic compounds found in naturally occurring physiologically relevant products that contains both natural and synthesized molecules with oxygen and nitrogen rings fused together. They have a number of key biological properties including anticancer activities [1], antimicrobial, insecticidal [2], anti-inflammatory [3] and molluscicidal activities [4]. The agricultural sector uses pyranopyrazole-based chemicals as herbicides, fungicides and insecticides [5].

Multicomponent reactions (MCRs) are one-pot processes in which at least three or more compounds react together to form the target product without the need for intermediate separation and purification. The main advantages of multicomponent reactions (MCRs) over traditional multistep protocols include higher efficiency, experimental simplicity, lower cost, reduced reaction time, minimal labour requirements and significantly decreased waste generation [6]. Based on the broad spectrum of biological activities associated with pyranopyrazole scaffolds, various synthetic strategies have been explored to efficiently construct these heterocyclic frameworks [7]. Combining MCR strategies with green protocols, such as conducting reactions in water, has gained significant interest [8-11]. Water is an attractive solvent due to its eco-friendliness, high cohesive energy density, negative activation volume and ability to stabilize the transition states through hydrogen bonding [12]. This MCR reaction has been widely explored with various catalysts such as acid catalysts *i.e*. silicotungstic acid [13], sodium salt of diethyloxaloacetate [14], high thermal heteropoly acid (HPA, $H_{14}NaP_5W_{30}O_{120}$) [15], base catalysts *i.e*. K_2CO_3, Et_3N, Et_2NH, pyrrolidine, piperidine, morpholine, piperazine [16], ionic liquids [17], resin bound polymeric catalysts [18], inorganic catalysts [19], organocatalysts [20], ultrasonic irradiation using nanoparticles [12], $CuSnO_3$:SiO_2 catalyst [22], microwave-assisted reactions with different catalysts and also in catalyst-free conditions.

This study reports the synthesis of 1,4-dihydropyrano[2,3-*c*]-pyrazole derivatives using L-histidine as a catalyst under two different conditions *viz*. (i) in water as a green solvent (**method I**) and (ii) under solvent-free conditions (**method II**),

employing the same catalyst. The physico-chemical properties, pharmacokinetic profiles, drug-likeness and medicinal chemistry aspects, such as lipophilicity and water solubility, were evaluated using the SwissADME web tool. Furthermore, inhibition potential against cytochrome P450 isoforms (CYP1A2, CYP2C19 and CYP2C9) was also assessed using SwissADME. Molecular docking studies were conducted using AutoDock and Molegro Molecular Viewer software. The synthesized compounds were docked against the bacterial target protein glucosamine-6-phosphate synthase (GlmS) (PDB ID: 2POC), which plays a crucial role in the bacterial cell wall biosynthesis. The binding interactions between the ligands and the active site of GlmS were analyzed, demonstrating favorable binding affinities. The results suggest that the synthesized pyranopyrazole derivatives exhibit promising antibacterial activity against both Gram-positive and Gram-negative bacterial strains.

EXPERIMENTAL

Melting points of the synthesized compounds were determined using open capillary tubes on a digital melting point apparatus and are uncorrected. FT-IR spectra were recorded on an ABB Bomem MB 104 spectrometer using KBr pellets in the range of 4000-400 cm^{-1}. ^1H NMR spectra were obtained on a JOEL GSX-400 MHz spectrometer using $CdCl_3$ as solvent and tetramethylsilane (TMS) as the internal standard. while ^{13}C NMR spectra were obtained using a Bruker 100 MHz spectrometer. UV-visible absorption spectra were recorded in ethanol using a Shimadzu UV-vis spectrophotometer (model 160A) over a wavelength range of 200-1000 nm. Thin-layer chromatography (TLC) was performed on silica gel G for TLC with petroleum ether – ethyl acetate solvent system and visualized in the iodine chamber. The purity of all synthesized compounds was confirmed by consistent TLC profiles and sharp melting points.

General procedure for synthesis of pyranopyrazole in water medium (method I): In a 100 mL flat-bottom flask, ethyl acetoacetate (10 mmol) and hydrazine hydrate (10 mmol) were added and stirred for 2-3 min. Subsequently, water (15 mL), malononitrile (10 mmol), aromatic aldehyde (10 mmol), and a catalytic amount of L-histidine (as specified in Table-1) were introduced into the reaction mixture. The reaction was carried out under reflux at 85 ºC with continuous stirring, and its progress was monitored by TLC until completion (**Scheme-I**).

TABLE-1
QUANTITY AND IMPACT ON
SYNTHESIS OF PYRANOPYRAZOLE

Entry	Catalyst (mol %)	Grinding time (min)	Yield (%)
1	0	35	50
2	5	20	65
3	10	15	83
4	15	5	92
5	20	5	92

General procedure for synthesis of pyranopyrazole in solvent free technique (method II): In a mortar, aromatic aldehyde (10 mmol), malononitrile (10 mmol), hydrazine hydrate (10 mmol), ethyl acetoacetate (10 mmol) and L-histidine (15 mol% relative to 10 mmol) were mixed. The mixture was ground using a mortar and pestle at different durations (Table-2), with reaction progress monitored by TLC. After an intermediate melt was observed, the solid product was allowed to stand for 5-10 min at room temperature. The resulting mixture was then transferred into ice-cold water, filtered and the crude product was purified by recrystallization from ethanol (**Scheme-I**).

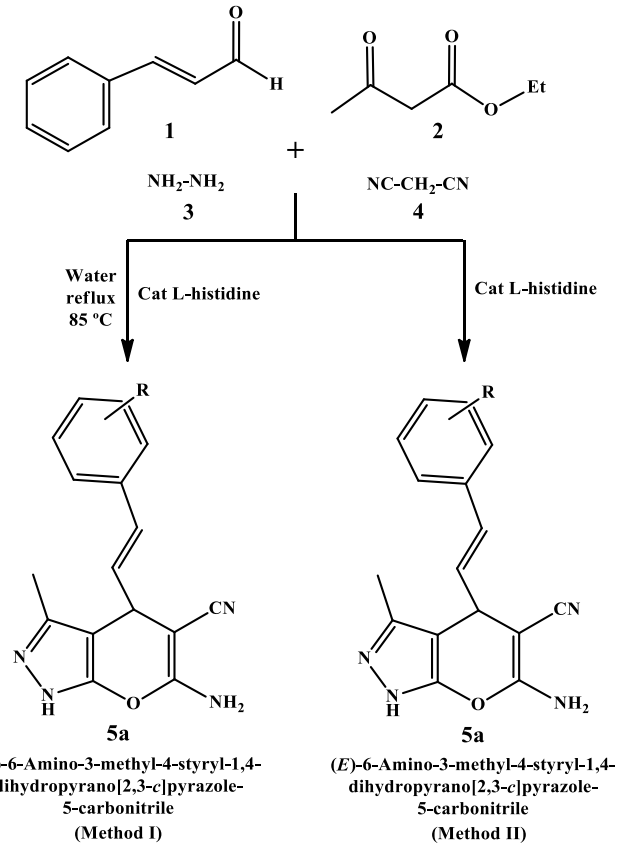

Scheme-I: Synthesis of (*E*)-6-amino-3-methyl-4-styryl-1,4-dihydro-pyrano-[2,3-*c*]pyrazole-5-carbonitrile using water medium and solvent free conditions

TABLE-2
OPTIMIZING THE REACTION TIME
AND PERCENTAGE OF YIELD (**5a-e**)

Compd.	Method I		Method II	
	Conventional reaction time (h)	Yield (%)	Grinding reaction time (min)	Yield (%)
5a	1.0	93	5	92
5b	1.5	92	4	90
5c	1.5	90	5	91
5d	1.0	92	4	90
5e	1.0	91	4	91

(*E*)-6-Amino-3-methyl-4-styryl-1,4-dihydropyrano-[2,3-*c*]pyrazole-5-carbonitrile (5a): A mixture of aromatic aldehyde (**1**), ethyl acetoacetate (**2**), hydrazine (**3**), malononitrile (**4**) and catalyst L-histidine taken in equal ratio (10 mmol) and performed both in water media as well as in grinding method gives yield 93% and 92%, respectively. Yellow solid,

m.p.: 179 ºC; FT-IR (KBr, ν_{max}, cm^{-1}): 3420, 3379, 2180, 1637, 1227, 1154, 749. ^{1}H NMR (400 MHz, DMSO-d_6, δ ppm): 2.21 (3H, s), 4.14 (1H, d, *J* = 4.6 Hz), 6.38-6.56 (2H, 6.46 (dd, *J* = 17.0, 4.6 Hz), 6.49 (d, *J* = 17.0 Hz), 6.51 (s, 2H, NH_2), 7.19 (1H, tt, *J* = 7.7, 1.3 Hz), 7.25-7.46 (4H, 7.33 (dddd, *J* = 7.7, 7.6, 1.8, 0.5 Hz), 7.39 (dddd, *J* = 7.6, 1.8, 1.3, 0.5 Hz); ^{13}C NMR (100 MHz, DMSO-d_6, δ ppm): 9.8 (1C, s), 73.2 (1C, s), 99.5 (1C, s), 113.2 (1C, s), 119.4 (1C, s), 126.5 (2C, s), 128.1 (1C, s), 128.7 (2C, s), 133.4 (1C, s), 135.6 (1C, s), 136.1 (1C, s), 141.3 (1C, s), 154.8 (1C, s), 160.9 (1C, s).

(*E*)-6-Amino-4-(4-chlorostyryl)-3-methyl-1,4-dihydropyrano[2,3-*c*]pyrazole-5-carbonitrile (5b): Yield: 92% (water media) and 90% (grinding method). Brown solid, m.p.: 176 ºC, FT-IR (KBr, ν_{max}, cm^{-1}): 3430, 3381, 2185, 1640, 1220, 1156, 739; ^{1}H NMR (400 MHz, DMSO-d_6, δ ppm): 2.21 (3H, s), 4.14 (1H, d, *J* = 4.6 Hz), 6.38-6.64 (2H, 6.46 (dd, *J* = 17.0, 4.6 Hz), 6.57 (d, *J* = 17.0 Hz), 6.59 (s, 2H, NH_2), 7.26 (2H, ddd, *J* = 8.0, 1.8, 0.5 Hz), 7.45 (2H, ddd, *J* = 8.0, 1.5, 0.5 Hz); ^{13}C NMR (100 MHz, DMSO-d_6, δ ppm): 9.8 (1C, s), 73.2 (1C, s), 99.5 (1C, s), 113.2 (1C, s), 119.4 (1C, s), 128.8 (2C, s), 129.1 (2C, s), 133.4 (1C, s), 134.6 (1C, s), 134.8 (1C, s), 135.6 (1C, s), 141.3 (1C, s), 154.8 (1C, s), 160.9 (1C, s).

(*E*)-6-Amino-3-methyl-4-(2-nitrostyryl)-1,4-dihydropyrano[2,3-*c*]pyrazole-5-carbonitrile (5c): Yield: 90% (water media) and 91% (grinding method). Brown solid, m.p.: 180 ºC, FT-IR (KBr, ν_{max}, cm^{-1}): 3429, 3372, 2187, 1635, 1224, 1150, 741. ^{1}H NMR (400 MHz, DMSO-d_6, δ ppm): 2.21 (3H, s), 4.53 (1H, d, *J* = 4.7 Hz), 6.72-6.94 (2H, 6.80 (dd, *J* = 15.5, 4.7 Hz), 6.58 (s, 2H, NH_2), 6.87 (d, *J* = 15.5 Hz), 7.46-7.74 (3H, 7.53 (ddd, *J* = 8.5, 7.7, 1.3 Hz), 7.60 (ddd, *J* = 7.7, 7.6, 2.1 Hz), 7.67 (ddd, *J* = 7.6, 1.3, 0.5 Hz), 8.07 (1H, ddd, *J* = 8.5, 2.1, 0.5 Hz). ^{13}C NMR (100 MHz, DMSO-d_6, δ ppm): 9.8 (1C, s), 73.2 (1C, s), 99.5 (1C, s), 113.2 (1C, s), 119.4 (1C, s), 124.9 (1C, s), 128.4 (1C, s), 129.2 (1C, s), 132.2 (1C, s), 132.6 (1C, s), 133.7 (1C, s), 135.6 (1C, s), 141.3 (1C, s), 148.0 (1C, s), 154.8 (1C, s), 160.9 (1C, s).

(*E*)-6-Amino-4-(2-hydroxystyryl)-3-methyl-1,4-dihydropyrano[2,3-*c*]pyrazole-5-carbonitrile (5d): Yield: 92% (water media) and 90% (grinding method). Pale yellow solid, m.p.: 202 ºC, FT-IR (KBr, ν_{max}, cm^{-1}): 3422, 3383, 2185, 1633, 1225, 1152, 74; ^{1}H NMR (400 MHz, DMSO-d_6, δ ppm): 2.21 (3H, s), 3.99 (1H, d, *J* = 3.8 Hz), 6.33-6.49 (2H, 6.41 (dd, *J* = 17.0, 3.8 Hz), 6.42 (d, *J* = 17.0 Hz), 6.54 (s, 2H, NH_2), 6.73 (1H, ddd, *J* = 8.3, 1.7, 0.5 Hz), 7.03 (1H, ddd, *J* = 7.9, 7.5, 1.7 Hz), 7.19 (1H, ddd, *J* = 8.3, 7.5, 1.5 Hz), 7.44 (1H, ddd, *J* = 7.9, 1.5, 0.5 Hz); ^{13}C NMR (100 MHz, DMSO-d_6, δ ppm): 9.8 (1C, s), 73.2 (1C, s), 99.5 (1C, s), 113.2 (1C, s), 116.4 (1C, s), 119.4-119.5 (2C, 119.4 (s), 119.4 (s)), 121.0 (1C, s), 127.5 (1C, s), 132.2 (1C, s), 132.6 (1C, s), 135.6 (1C, s), 141.3 (1C, s), 154.8 (1C, s), 155.6 (1C, s), 160.9 (1C, s).

(*E*)-6-Amino-4-(2-bromostyryl)-3-methyl-1,4-dihydropyrano[2,3-*c*]pyrazole-5-carbonitrile (5e): Yield: 91% (water media) and 91% (grinding method). Yellow solid, m.p.: 209 ºC, FT-IR (KBr, ν_{max}, cm^{-1}): 3420, 3379, 2180, 1637, 1227, 1154, 749; ^{1}H NMR (400 MHz, DMSO-d_6, δ ppm): 2.21 (3H, s), 4.10 (1H, d, *J* = 4.4 Hz), 6.34-6.56 (2H, 6.42 (dd, *J* = 16.8, 4.4 Hz), 6.48 (d, *J* = 16.8 Hz), 6.53 (s, 2H, NH_2), 7.10 (1H, ddd, *J* = 8.0, 7.6, 1.5 Hz), 7.20-7.41 (3H, 7.27 (ddd, *J* = 7.8, 7.6, 1.1 Hz), 7.26 (ddd, *J* = 8.0, 1.1, 0.5 Hz), 7.35 (ddd, *J* = 7.8, 1.5, 0.5 Hz); ^{13}C NMR (100 MHz, DMSO-d_6, δ ppm): 9.8 (1C, s), 73.2 (1C, s), 99.5 (1C, s), 113.2 (1C, s), 119.4 (1C, s), 123.4 (1C, s), 126.7 (1C, s), 127.5 (1C, s), 129.6 (1C, s), 132.2 (1C, s), 133.0 (1C, s), 135.6 (1C, s), 136.3 (1C, s), 141.3 (1C, s), 154.8 (1C, s), 160.9 (1C, s).

Antibacterial activity: To evaluate the antibacterial efficacy, microbial inocula were evenly spread on the agar plates, and wells were aseptically bored for test and standard solutions. Plates were incubated according to the microorganisms tested, allowing diffusion of antibacterial agents into the agar, which inhibits microbial growth. All the synthesized pyranopyrazole derivatives (**5a-e**) were tested against human pathogenic bacteria including *Escherichia coli*, *Staphylococcus aureus*, *Staphylococcus epidermidis*, *Pseudomonas aeruginosa*, *Klebsiella oxytoca* and *Bacillus subtilis* (procured from the National Centre for Microbial Resource (NCMR), National Centre for Cell Science (NCCS), Pune, India), using amikacin as a standard reference. Antibacterial activity was assessed by the agar well diffusion method and minimum inhibitory concentration (MIC). Paper discs containing 1.0% w/v test compounds and methanol (control) were applied to inoculated agar plates and incubated at 37°C for 48 h [23]. The diameter of the inhibition zone (IZ, in mm) was measured to determine the activity.

ADMET parameters: The SwissADME web tool was employed to evaluate the synthesized compounds (**5a-e**) for their physico-chemical properties, pharmacokinetic profiles, drug-likeness and medicinal chemistry aspects, including lipophilicity and water solubility. The 2D molecular structures were converted into SMILES format, facilitating efficient and rapid virtual screening. SwissADME, a freely accessible platform (http://www.swissadme.ch/), provides a user-friendly interface for assessing the drug-like behaviour of small molecules and identifying potential candidates for further development [24-27].

Ligand preparation and MM2 optimization: The pyranopyrazole derivatives were sketched using ChemDraw and converted to 3D structures with the help of Chem3D software. Molecular mechanics (MM2) force field calculations were applied to optimize the geometry, predict molecular energy and ensure a stable conformation suitable for docking. The optimized structures revealed three aromatic π-systems within the synthesized molecules. Significant van der Waals (VDW) interactions were observed between atoms 1–5 (R = 3.340 Å) and 15–28 (R = 2.510 Å), with a total calculated energy of 94.318 kcal/mol (Table-3). MM2 optimization helped to confirm the structural stability of the ligands, supporting the reliability of subsequent docking studies.

TABLE-3
MM2 ENERGY CALCULATION

Stretch	0.9195
Bend	12.6458
Stretch-bend	-0.0829
Torsion	-10.2172
Non-1,4 VDW	-2.7794
1,4 VDW	12.1997
Dipole/dipole	3.4620
Total energy	16.1474 kcal/mol

Protein preparation: The crystal structure of glucosemine-6-phosphate synthase (GlmS) (PDB ID: 2POC) was retrieved from the Protein Data Bank (www.rcsb.org). GlmS was selected due to its essential role in the bacterial cell wall biosynthesis, making it a promising antibacterial target. Prior to docking, water molecules were removed and hydrogen atoms were added to complete the protein structure. Protein preparation and active site prediction were performed using Discovery Studio Visualizer, which identified the binding pocket for ligand interaction.

Molecular docking: AutoDock software was used to perform the molecular docking studies. This process was carried out to determine the interactions and binding affinities of the optimized ligands and glucose-6-phosphate synthase. The active region of protein has been identified using a 20 × 20 × 20 Å grid box. After the docking process was completed, the results were assessed using the docking scores, which indicate the ligands' binding affinities to the protein and Discovery Studio Visualizer was used to view and analyse the protein-ligand complexes.

RESULTS AND DISCUSSION

Pyranopyrazole synthesis has been reported under various catalytic conditions; however, many approaches suffer from low yields, the use of toxic catalysts, harsh reaction conditions, or hazardous solvents. In this work, L-histidine is introduced as a green catalyst for both solvent-free and water-mediated synthesis of pyranopyrazoles. A control reaction without catalyst showed no product formation after 1.5 h. The use of 2.5 mol% L-histidine yielded 80%, while increasing the catalyst loading to 10 mol% improved the yield to 93%; further increases had no significant effect. Initially (method II), cinnamaldehyde, malononitrile and ethyl acetoacetate were ground with L-histidine in a solvent-free environment. Without a catalyst, the product was not produced after 25 min of grinding. But in the presence of L-histidine, the reaction proceeds with less time duration. Increasing the L-histidine loading to 5, 10, 15 and 20 mol% improved the product yields to 65%, 83%, 92% and 92%, respectively, with corresponding solidification times of 20, 15, 5, and 5 min (Table-1).

The FT-IR spectrum exhibited characteristic absorption peaks at 3420 and 3379 cm^{-1}, corresponding to N–H and O–H stretching vibrations, indicating the presence of hydroxyl and amino groups, respectively. A sharp peak at 2180 cm^{-1} is attributed to the stretching vibration of the cyano (–CN) group. The strong absorption at 1637 cm^{-1} corresponds to the C=C and C=O stretching, confirming the presence of conjugated carbonyl and alkene functionalities within the heterocyclic ring system. Peaks at 1227 and 1154 cm^{-1} are due to C–N and C–O stretching vibrations, while the peak at 749 cm^{-1} indicates aromatic C–H out-of-plane bending. In ^{1}H NMR, the aromatic peaks observed in the region of 6.38-6.56 ppm. The broad singlet observed at 6.56 ppm for NH_2, a doublet at 4.14 ppm and doublet of doublet at 6.46 ppm confirms the aldehyde ring to form 1,4-dihydropyranopyrazole. The ^{13}C NMR spectra of compounds **5a-e** confirmed the formation of the dihydropyrano[2,3-*c*]pyrazole scaffold, as evidenced by consistent chemical shifts across the synthesized series. All compounds exhibited a characteristic signal around 9.8 ppm, corresponding to the methyl group on the pyrazole ring. A signal at ~73.2 ppm was observed for the methine carbon, confirming the presence of the fused pyran ring. The signal at ~99.5 ppm is attributed to the C-4a quaternary carbon of the pyran moiety, while resonances between 113-141 ppm represent various aromatic carbons, showing slight shifts depending on the nature and position of substituents on the phenyl ring. Downfield signals around 154.8 ppm and 160.9 ppm are assigned to the electron-deficient carbons in the pyrazole and pyran rings, respectively, indicative of conjugated keto and imine functionalities. Finally, the variations among derivatives (**5b-e**) in the aromatic region (120-140 ppm) reflect different substitution patterns, which is especially evident in compounds **5d** and **5e**, where additional electron-donating or electron-withdrawing groups cause slight deshielding or shielding effects. Furthermore, the UV-visible spectrum displayed a broad absorption band at 230 nm, characteristic of π-π* transitions within the conjugated pyranopyrazole system, further supporting the formation of the fused heterocyclic ring.

Mechanism: Pyranopyrazole derivatives are synthesized by the Knoevenagel condensation of aldehyde molecules and malononitrile, yielding intermediate I. The reaction takes place simultaneously with the formation of intermediate II derived from phenylhydrazine and ethylacetoacetate precursors. Subsequently, the Michael addition and cyclization of the intermediate I and II lead to the formation of a pyranopyrazole(1,4-dihydropyrano[2,3-*c*]pyrazole derivative (**Scheme-II**).

Antibacterial activity: The synthesized pyranopyrazole derivatives (**5a-e**) were evaluated against six bacterial strains using the agar well diffusion method. Compounds **5a** and **5c** exhibited the most significant antibacterial activity, showing the inhibition zones comparable to or exceeding amikacin (standard drug). Notably, compound **5a** showed strong activity against *K. oxytoca* (26 mm) and *P. aeruginosa* (24 mm), while compound **5c** was highly effective against *S. epidermidis* (25 mm) and *E. coli* (21 mm). The other compounds **5b**, **5d** and **5e** showed moderate to low activity, with **5e** being the least effective across all strains. The results suggest that compounds **5a** and **5c**, such as electron-withdrawing groups and improved solubility, may enhance bacterial cell penetration and binding affinity to microbial targets.

ADMET parameters: Table-4 presents key ADMET-related physico-chemical properties of compounds **5a-e**. All compounds have molecular weights below 500 g/mol and Log P values between 1.59 and 2.92, indicating favourable lipophilicity and good potential for oral bioavailability. The number of hydrogen bond acceptors (3–5) and donors (2–3) also comply with Lipinski's rule of five, supporting good membrane permeability and solubility. Significantly, compound

TABLE-4
ADMET PROPERTIES OF SYNTHESIZED COMPOUNDS **5a-e**

Compd.	MM	Log P	H-Bond acceptor	H-Bond donor
5a	278.31 g/mol	2.31	3	2
5b	312.75 g/mol	2.87	3	2
5c	323.31 g/mol	1.59	5	2
5d	294.31 g/mol	1.90	4	3
5e	357.20 g/mol	2.92	3	2

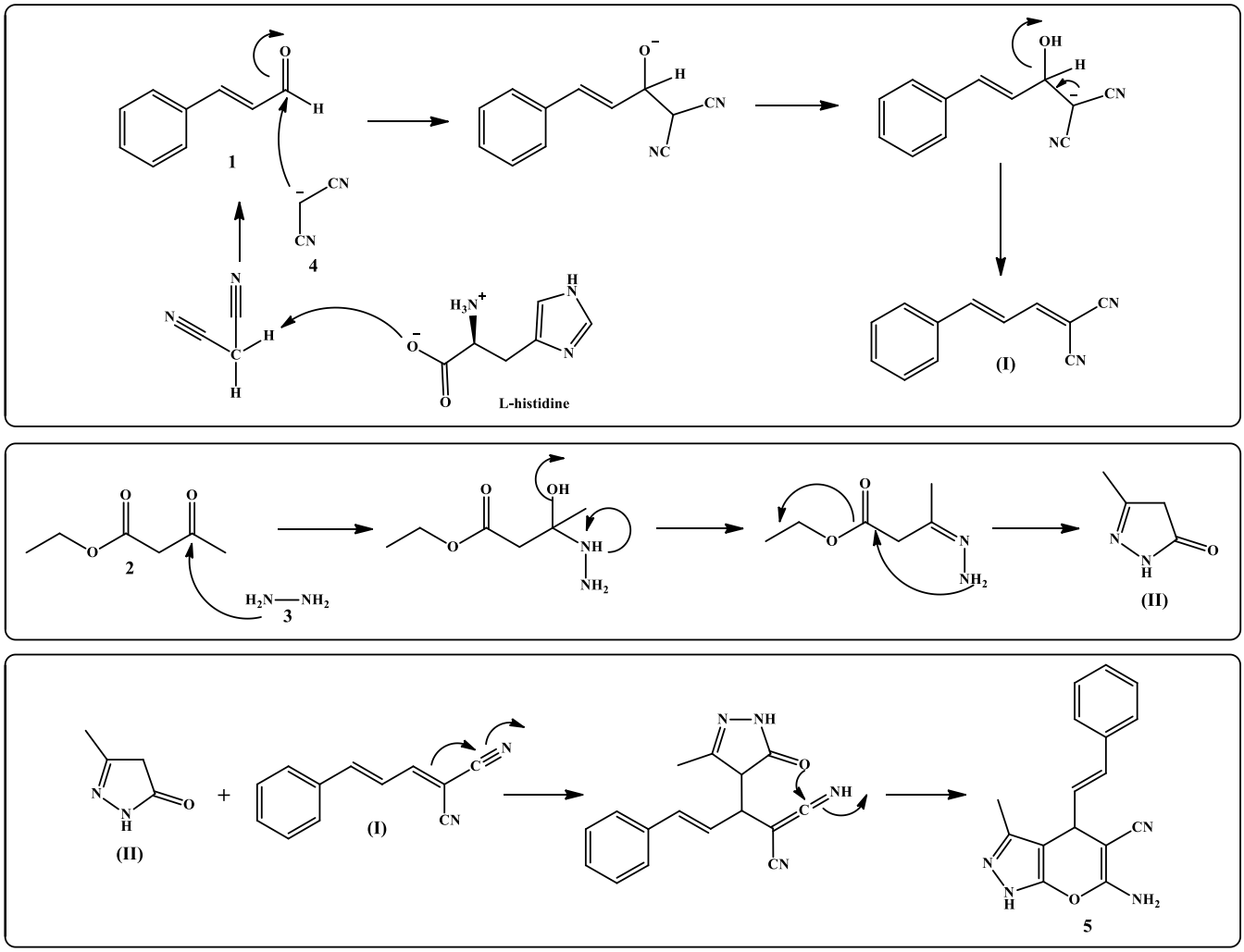

Scheme-II: Mechanism route of synthesis of 1,4-dihydropyrano[2,3-*c*]pyrazole

5c shows the highest solubility potential due to its lower Log P and higher number of hydrogen bond acceptors.

In silico ADME analysis revealed that all the synthesized compounds (**5a-e**) exhibit high gastrointestinal (GI) absorption, suggesting good potential for oral bioavailability (Table-5). The cytochrome P450 enzymes, CYP1A2, CYP2C19, and CYP2C9, are key players in drug metabolism, and the evaluated ADME profiles indicate that compounds **5a-e** may interact with these enzymes, supporting their relevance in early-stage drug discovery. Furthermore, none of the compounds violated the major drug-likeness rules, including those proposed by Lipinski, Muegge, Ghose, Veber and Egan, confirming their compliance with established drug-likeness criteria (Table-6). The presence of one rotatable bond in these molecules also suggests favorable water solubility and the potential to cross the blood–brain barrier (BBB). Among the tested compounds, compounds **5a**, **5b** and **5e** were predicted to inhibit CYP1A2, CYP2C19, and CYP2C9, indicating possible implications in drug-drug interactions and metabolism. Furthermore, all the synthesized compounds exhibited good aqueous solubility. Notably, compound **5c** was fully water-soluble, showed high biological permeability, and inhibited CYP2C9. It also had the lowest Log Kp value (–6.29 cm/s), indicating minimal potential for transdermal absorption.

Molecular docking: AutoDock docking results revealed that glucosamine-6-phosphate synthase (GlmS), a critical enzy-

TABLE-5
PHARMOKINETIC PROPERTIES FROM ADME

Compd.	GI abs.	BBB pen.	P-gp sub.	CYP1A2	CYP2C19	CYP2C9	CYP2D6	CYP3A4	Log Kp (skin permeability)
5a	High	No	No	Yes	Yes	Yes	No	No	-5.90 cm/s
5b	High	No	No	Yes	Yes	Yes	No	No	-5.66 cm/s
5c	High	No	No	No	No	Yes	No	No	-6.29 cm/s
5d	High	No	No	Yes	No	No	No	No	-6.24 cm/s
5e	High	No	No	Yes	Yes	Yes	No	No	-5.88 cm/s

TABLE-6
DRUGLIKENESS FROM ADME

Compound	Lipinski	Ghose	Veber	Egan	Muegee	Bioavailability score
5a	Yes	Yes	Yes	Yes	Yes	0.55
5b	Yes	Yes	Yes	Yes	Yes	0.55
5c	Yes	Yes	Yes	No	Yes	0.55
5d	Yes	Yes	Yes	Yes	Yes	0.55
5e	Yes	Yes	Yes	Yes	Yes	0.55

me in bacterial cell wall synthesis, binds strongly with the ligand **5a**. This interaction suggests ligand **5a**'s potential as an effective inhibitor against multiple bacterial strains, as supported by *in vitro* antibacterial activity summarized in Table-7. Five distinct binding pockets were identified within the protein, with ligand **5a** engaging multiple cavities (Fig. 1). The ligand demonstrated a high Vina docking score alongside significant cavity volumes (Table-8), indicating strong binding affinity and optimal structural compatibility. These findings underscore the importance of ligand **5a** in inhibiting GlmS and highlight its promise as a lead compound for the antibacterial drug development.

Conclusion

A green and efficient one-pot four-component synthesis of pyranopyrazole derivatives (**5a-e**) was achieved using L-histidine as a catalyst under both solvent-free and aqueous conditions. High yields (above 90%) were obtained, with the solvent-free grinding method obtaining the product within just 5 min. Structural confirmation was carried out using UV-

TABLE-7
INHIBITORY ZONE VALUE (mm) OF SEVERAL BACTERIAL STRAINS

Compound	*Staphylococcus aureus*	*Staphylococcus aureus*	*Staphylococcus epidermidis*	*Pseudomonas aeruginosa*	*Klebsiella oxytoca*	*Bacillus subtilis*
5a	20	22	26	24	26	23
5b	18	24	20	20	22	18
5c	21	21	25	24	22	22
5d	17	13	19	13	17	18
5e	12	18	17	15	16	13

Standard disc: Amikacin 18

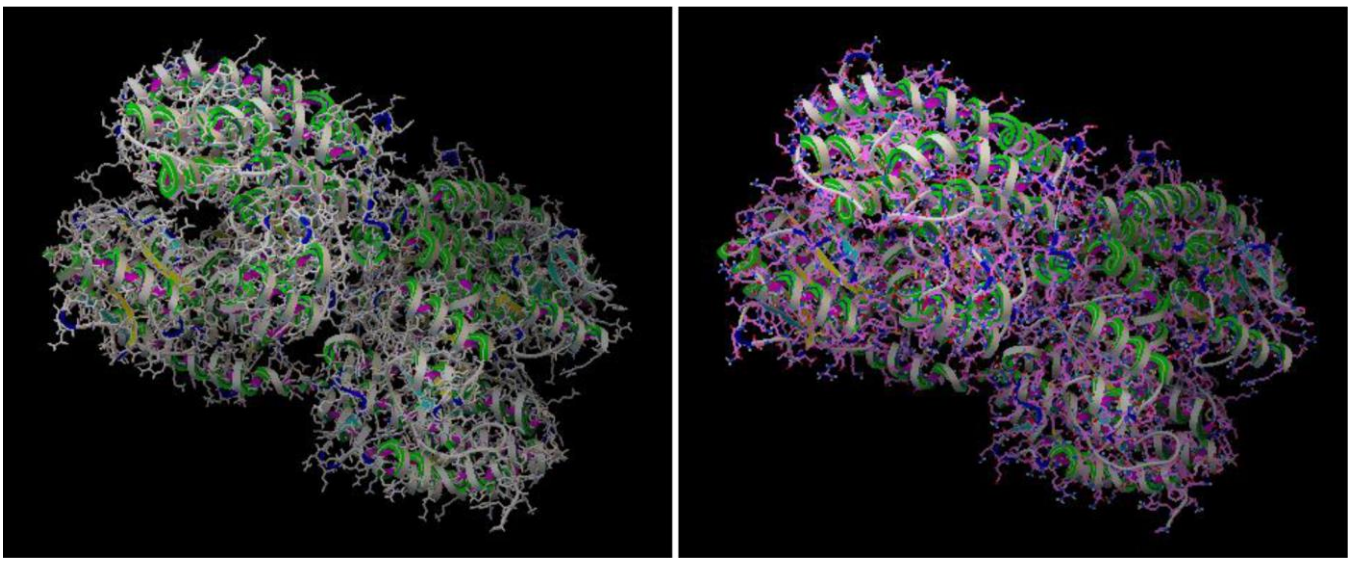

Fig. 1. The binding between protein and the synthesized ligand **5a**

TABLE-8
CAVITY AND DOCKING RESULTS OF THE SYNTHESIZED LIGAND **5a** WITH THE PROTEIN (2POC)

CurPocket ID	Vina score	Cavity volume (Å^3)	Center (x, y, z)	Docking size (x, y, z)
C4	-8.3	1484	52, -15, 74	21, 21, 21
C5	-8.1	1119	53, 15, 93	21, 21, 21
C1	-7.9	4869	49, -6, 91	34, 32, 21
C2	-7.8	4403	50, -27, 56	35, 21, 21
C3	-7.4	1600	56, -46, 54	21, 21, 27

Vis, FT-IR, ^{1}H and ^{13}C NMR analyses. SwissADME analysis revealed that the synthesized compounds inhibit key cytochrome P450 enzymes (CYP1A2, CYP2C19 and CYP2C9), indicating strong potential for oral drug development. Molecular docking studies using AutoDock showed favourable binding energies and Vina scores between the synthesized ligands and glucosamine-6-phosphate synthase (GlmS), a validated antibacterial target. The binding interactions also support the compounds' potential to act as effective antibacterial agents against both Gram-positive and Gram-negative strains.

CONFLICT OF INTEREST

The authors declare that there is no conflict of interests regarding the publication of this article.

REFERENCES

1. A.H.F. Abdelwahab, R.M.A. Borik, A.A. Alamri, H.M. Mohamed, M.S. Mostafa, A.A.M. Al-Dies, K.S. Ismail and A.A. Elhenawy, Anti-Cancer Agents Med. Chem., 25, 1253 (2025); https://doi.org/10.2174/0118715206376210250319053528
2. S.A.M. Abdelgaleil and Y.M. Badawy, *Alexandria Sci. Exchan. J.*, **37**, 572 (2016).
3. A.M. Malebari, H.E.A. Ahmed, S.K. Ihmaid, A.M. Omar, Y.A. Muhammad, S.S. Althagfan, N. Aljuhani, A.A.A. El-Sayed, A.H. Halawa, H.M. El-Tahir, S.A. Turkistani, M. Almaghrabi, A.K.B. Aljohani, A.M. El-Agrody and H.S. Abulkhair, *Bioorg. Chem*., **130**, 106255 (2023); https://doi.org/10.1016/j.bioorg.2022.106255
4. F.M. Abdelrazek, P. Metz, N.H. Metwally and S.F. El-Mahrouky, *Arch. Pharm.*, **339**, 456 (2006); https://doi.org/10.1002/ardp.200600057
5. S. Farooq and Z. Ngaini, *ChemistrySelect*, **9**, e202400028 (2024); https://doi.org/10.1002/slct.202400028
6. M. Mamaghani and R. Hossein Nia, *Polycycl. Aromat. Compd.*, **41**, 223 (2021); https://doi.org/10.1080/10406638.2019.1584576
7. R.K. Ganta, N. Kerru, S. Maddila and S.B. Jonnalagadda, *Molecules*, **26**, 3270 (2021); https://doi.org/10.3390/molecules26113270
8. C. Li and T. Chan, Organic Reactions in Aqueous Media, Wiley: New York, NY (1997).
9. R.C. Cioc, E. Ruijter and R.V.A. Orru, *Green Chem*., **16**, 2958 (2014); https://doi.org/10.1039/C4GC00013G
10. K. Kandhasamy and V. Gnanasambandam, *Curr. Org. Chem.*, **13**, 11820 (2009).
11. C. Z. Andrade and L. Alves, *Curr. Org. Chem.*, **9**, 195 (2005); https://doi.org/10.2174/1385272053369178
12. M. Cortes-Clerget, J. Yu, J.R.A. Kincaid, P. Walde, F. Gallou and B.H. Lipshutz, *Chem. Sci.*, **12**, 4237 (2021); https://doi.org/10.1039/d0sc06000c
13. H.V. Chavan, S.B. Babar, R.U. Hoval and B.P. Bandgar, *Bull. Korean Chem. Soc.*, **32**, 3963 (2011); https://doi.org/10.5012/bkcs.2011.32.11.3963
14. V.L. Gein, T.M. Zamaraeva and P.A. Slepukhin, *Tetrahedron Lett.*, **55**, 4525 (2014); https://doi.org/10.1016/j.tetlet.2014.06.077
15. R. Hekmatshoar, M.M. Heravi, S. Sadjadi, H.A. Oskooie and F.F. Bamoharram, *Catal. Commun.*, **9**, 837 (2008); https://doi.org/10.1016/j.catcom.2007.09.007
16. G. Vasuki and K. Kumaravel, *Tetrahedron Lett.*, **49**, 5636 (2008); https://doi.org/10.1016/j.tetlet.2008.07.055
17. R.S. Aliabadi and N.O. Mahmoodi, *RSC Adv.*, **6**, 85877 (2016); https://doi.org/10.1039/C6RA17594E
18. A. Ahmad, S. Rao and S. Nitinkumar, *RSC Adv.*, **13**, 28798 (2023); https://doi.org/10.1039/D3RA05570A
19. M. Mamaghani and R. Hossein Nia, *Polycycl. Aromat. Compd.*, **41**, 223 (2021); https://doi.org/10.1080/10406638.2019.1584576.
20. M.M. Khan, B. Singh, A. Arif, Saigal and S.C. Sahoo, *Tetrahedron Green Chem.*, **4**, 100050 (2024); https://doi.org/10.1016/j.tgchem.2024.100050
21. A. Dandia, V. Parewa, A.K. Jain and K.S. Rathore, *Green Chem.*, **13**, 2135 (2011); https://doi.org/10.1039/c1gc15244k
22. S.L. Sangle, D.R. Tope, A.V. Borhade, S.S. Ghumar, *J. Adv. Sci. Res.*, **13**, 38 (2022).
23. F. Sevgi and A.D. Bedük, *World Appl. Sci. J.*, **19**, 192 (2012).
24. R. Dennington, T.A. Keith and J.M. Millam, GaussView 6.0. 16, Semichem Inc, Shawnee Mission, KS, USA (2016).
25. A.D. Becke, *J. Chem. Phys.*, **98**, 1372 (1993); https://doi.org/10.1063/1.464304
26. I. Ahmad, H. Khan and G. Serdaroglu, *Comput. Biol. Chem.*, **104**, 107861 (2023); https://doi.org/10.1016/j.compbiolchem.2023.107861
27. D. Mothay and K.V. Ramesh, *Virusdisease*, **31**, 194 (2020); https://doi.org/10.1007/s13337-020-00585-z